environments

MDPI

Article

Optical Monitoring of Particulate Matter: Calibration Approach, Seasonal and Diurnal Dependency, and Impact of Meteorological Vectors

Salma Zaim [1,2,3,*], Bouchra Laarabi [2], Hajar Chamali [2], Abdelouahed Dahrouch [4], Asmae Arbaoui [1,2], Khalid Rahmani [2], Abdelfettah Barhdadi [2] and Mouhaydine Tlemçani [3,*]

1 Thermodynamic Energy Laboratory (LTE), Faculty of Sciences, Mohammed V University in Rabat, Rabat 10000, Morocco; arbaoui_asmae@yahoo.fr
2 Physics of Semiconductors and Solar Energy Research Team (PSES), Energy Research Center (CRE), Ecole Normale Supérieure, Mohammed V University in Rabat, Rabat 10000, Morocco; laarabi.b@gmail.com (B.L.); abdelfettah.barhdadi@ens.um5.ac.ma (A.B.)
3 Instrumentation and Control Laboratory-LAICA, Center for Sci-Tech Research in Earth System and Energy-CREATE, University of Evora, 7000-671 Evora, Portugal
4 Royal Gendarmerie Forensic Science Institute, Rabat 10000, Morocco
* Correspondence: salma_zaim2@um5.ac.ma (S.Z.); tlem@uevora.pt (M.T.)

Abstract

The worldwide air pollution situation reveals significant environmental challenges. In addition to being a major contributor to the deterioration of air quality, particulate matter (PM) is also an important factor affecting the performance of solar energy systems given its ability to decrease light transmission to solar panels. As part of our research, the present investigation involves monitoring concentrations of PM using a high-performance optical instrument, the in situ calibration protocol of which is described in detail. For the city of Rabat, observations revealed significant variations in concentrations between day and night, with peaks observed around 8 p.m. correlating with high relative humidity and low wind speeds, and the highest levels recorded in February with a monthly average value reaching 75 $\mu m/m^3$. In addition, an experimental protocol was set up for an analysis of the elemental composition of particles in the same city using SEM/EDS, providing a better understanding of their morphology. To assess the impact of meteorological variables on PM concentrations in two distinct climatic environments, a database from the city of Marrakech for the year 2024 was utilized. Overall, the distribution of PM values during this period did not fluctuate significantly, with a monthly average value not exceeding 45 $\mu m/m^3$. The random forest method identified the most influential variables on these concentrations, highlighting the strong influence of the type of environment. The findings provide crucial information for the modeling of solar installations' soiling and for improving understanding of local air quality.

Keywords: air pollution; particulate matter; solar energy; meteorological variables; random forest

Academic Editor: Ching-Yuan Chang

Received: 22 April 2025
Revised: 11 June 2025
Accepted: 13 June 2025
Published: 16 July 2025

Citation: Zaim, S.; Laarabi, B.; Chamali, H.; Dahrouch, A.; Arbaoui, A.; Rahmani, K.; Barhdadi, A.; Tlemçani, M. Optical Monitoring of Particulate Matter: Calibration Approach, Seasonal and Diurnal Dependency, and Impact of Meteorological Vectors. *Environments* **2025**, *12*, 244. https://doi.org/10.3390/environments12070244

1. Introduction

1.1. Background

Suspended particulate matter, commonly known as PM, is currently the focus of attention in many areas of activity [1]. It represents a major challenge to public health and the environment [2]. It refers to tiny solid or liquid particles suspended in the air, classified

according to their diameter [3]. The sources of particulate matter are diverse, including human activities such as industry, transport, agriculture, and fossil fuel combustion, as well as natural processes such as volcanic eruptions, forest fires, sandstorms, and dust transport [4]. Moreover, these particles may be derived from atmospheric transformations incorporating dilution, coagulation, condensation, and deposition [5]. The finer particles tend to be present in very large numbers but are rarely captured in mass concentration measurements due to their very low mass [6].

From a historical perspective, since the 1990s, air quality monitoring networks have focused primarily on the concentrations of PM10 (particulates $\leq$ 10 µm in diameter) in ambient air [7]. Accordingly, in 1999, the European Directive 1999/30/EC set limit values for PM10, marking a milestone in their regulatory consideration [8]. Since the 2000s, measurements of PM2.5 (particulates $\leq$ 2.5 µm in diameter) have also been developed, considering these fine particles to be a more relevant indicator of health effects. Currently, PM10 and PM2.5 concentrations are systematically included in the calculation of the Air Quality Index (AQI) [9].

Counting measurements allow for the identification of these very fine particles and improve our knowledge of aerosol origins and formation mechanisms [10,11]. The characterization of aerosol numbers is generally associated with the study of their granulomere distribution, which refers to their number distribution according to different size classes [12–14]. Furthermore, aerosol particle size distribution is one of the most critical physical parameters of aerosols [15,16]; it defines the aerosol sedimentation velocities and lifetime in the atmosphere and largely controls the aerosol radiative effect. Although many studies have addressed the impacts of PM on human health, visibility, and other atmospheric aspects [17], relatively limited attention has been devoted to the combined effect of PM on solar irradiance—a major element in the solar energy production process—particularly in terms of their concentration, deposition rate, nature, and morphology. This effect on the performance of these systems is manifested not only by the attenuation of the amount of solar irradiance reaching solar panels but also the accumulation of the particles on the surfaces of solar installations, leading to a phenomenon known as soiling [18]. When suspended fine particles such as PM accumulate on solar panels, they decrease their efficiency by reducing light transmission [19]. The dust cycle, relating to the process of soiling, follows several stages from elaboration to elimination, as detailed below and represented in Figure 1:

- **Emission:** This is the first phase of the soiling process referring to the generation and release of particles into the environment originating from a variety of sources, including industrial activities, road traffic, and local climatic circumstances. When emitted into the atmosphere, particulates are transported by the wind according to their size and weight.
- **Deposition:** While gravitational settling is a significant driver, it is not the only mechanism involved. Inertial impact caused by particles in turbulent airflows also plays a big role, particularly for larger particles that deviate from streamlines and collide with surfaces. In addition, interception occurs when particles follow airflow lines that bring them close enough to surfaces for them to adhere.
- **Interaction:** These refer to the forces that retain the particles on the surface. The deposited particles interact with the surface of the solar panels through several physical and chemical forces, affecting their adhesion and resistance to removal. These include Van der Waals forces—responsible for the initial adhesion of fine particles to the solar panel surface. In addition, cementation refers to a process where particles are permanently bonded to the panel surface due to the formation of strong chemical or physical bonds, often under exposure to moisture or heat.

- **Removal:** Particles can be eliminated from solar panels by a number of natural and artificial mechanisms. Manual or mechanical cleaning is one of the most common methods. Wind also has a significant role to play in the natural removal of light particles. The cleaning process is also driven by rain. However, this effect is generally more noticeable when precipitation is heavy since short or light rain may not provide sufficient flow to effectively remove adhering dust.

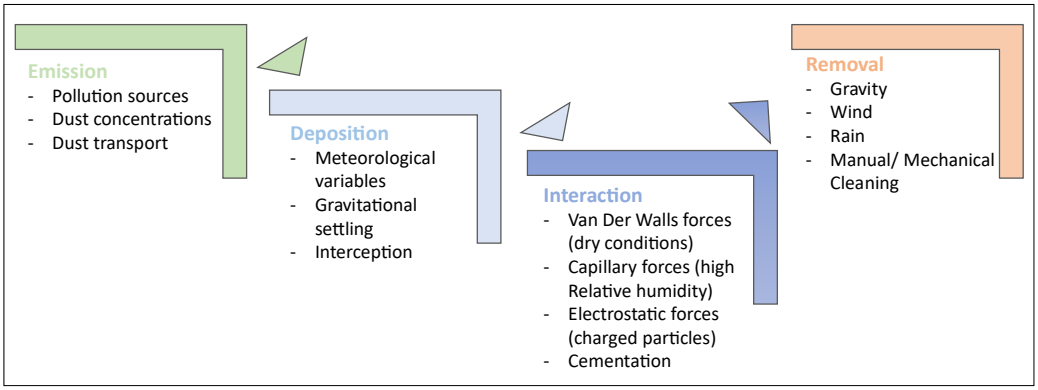

Figure 1. Dust cycle description for solar panel surfaces.

1.2. Context and Objective of This Study

For many applications, the monitoring of suspended PM represents a critical issue. The information concerning the concentration of suspended particles remains largely unavailable or fragmented, making it difficult to accurately assess air pollution in various regions of the country [20]. This gap in data collection is an obstacle to understanding the environmental impacts associated with air pollution [21–23]. For this reason, it is essential to initiate targeted studies to fill this information deficit.

One of the measuring instruments that are used for the monitoring of PM is the DustTrak DRX. It is a light-scattering laser photometer that is specially designed to provide high precision, real-time measurements of particle concentrations, setting it apart from other instruments. Its advanced technology enables accurate detection, even at low concentrations [24]. However, calibrating such an instrument is a pivotal process in ensuring accuracy and reliability of the data collected. Indeed, its precision can vary depending on the environment in which it is used. Unfortunately, there is no clearly defined standardized calibration methodology for this device under specific conditions. This unavailability of a reference can potentially lead to biases in the measurements, complicating the comparison of results between different sites. In this respect, the on site calibration operation becomes crucially relevant as it allows the instrument to identify and adapt its measurements to the characteristics of the local environment.

Based on all that has been said, our study aims at the establishment of rigorous monitoring of suspended PM concentrations in Rabat City (Rabat, Morocco), using the DustTrak DRX measuring instrument. In addition, it provides a clear calibration methodology of this instrument for specific conditions and characterizes the composition of particles. Furthermore, a database with the same variables is used to compare the effect of meteorological variables on PM concentration in two different environments. This investigation intends to support future researchers in this field, inform experimental sampling decision-making, and provide a benchmark for PM measurement and monitoring. Concretely, it aims to answer the following questions: How are particles measured? What does an optical monitor calibration protocol consist of? Which trends are observed in PM concentrations in the city of Rabat? How do meteorological variables affect PM concentrations?

2. Materials and Methods

The methodological approach adopted to carry out the present study consisted of several key phases, as illustrated in the flowchart (Figure 2). The period for monitoring concentrations in Rabat City occurred from 3 January to 3 November 2023. For the data from the city of Marrakech, used for comparison, a database for the year 2024 from the AirNet network platform—also known as the "citizen science project of the sensor community" of the city of Marrakech—was retrieved and processed.

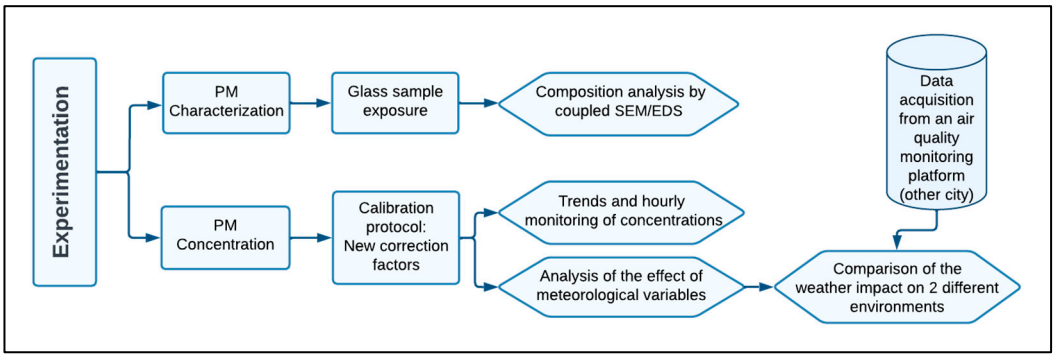

Figure 2. Experimental workflow.

Firstly, the instrumentation, which forms the basis of data collection, was set up. Next, a crucial calibration phase, ensuring that the instrument works accurately and reliably to measure particle concentrations, was performed before launching measurements to collect real-time data. This systematic approach was designed to ensure the scientific rigor of our study and to provide meaningful results for the analysis of air pollution by PM in Rabat. For the section on analyzing the importance of meteorological variables in relation to the behavior of PM concentrations, the random forest method was used on the Rabat and Marrakech data separately. In parallel, to address the question of determining what particles are, a sampling protocol was set up to sample particles on glass supports for physico-chemical analysis. It is worth mentioning that by analyzing the chemical composition of particles, it is possible to determine their origin—whether natural or anthropogenic.

2.1. Site Topography and Meteorological Conditions

This experimental study was carried out at the laboratory measurement platform located at the ENS "Ecole Normale Supérieure" in Rabat City, situated on the northwest Atlantic coast. According to the Köppen–Geiger climate ranking, the city is classified as a Csa type. The letter "C" stands for temperate climates, the "s" for dry summers, and "a" for wet winters. The site is located in an environment principally surrounded by residential areas and transport routes, while also benefiting from the presence of green spaces. Meteorological data for the city of Rabat were collected from the measuring station available on the roof of the laboratory (Figure 3), including sensors for temperature, humidity, wind speed/direction, precipitation, solar radiation, and many others.

Figure 3. Measurement chain located on the laboratory roof.

As shown in Figure 4, the key meteorological variables for the year 2023 vary from month to month. The maximum GHI value is 1179 W/m^2 in May, while the highest DHI value is 682.9 W/m^2 in June. The month of February was the coldest, with a minimum value of 6.85 °C, while the maximum temperature reached 43.25 °C in June. Concerning wind patterns, the city of Rabat is often influenced by sea winds, given its position on the Atlantic coast. Typically, winds in this region tend to come from the west or northwest, bringing a cool breeze. The maximum wind speed is 11.19 m/s during October, which features the highest amount of rainfall at 42.6 mm/month.

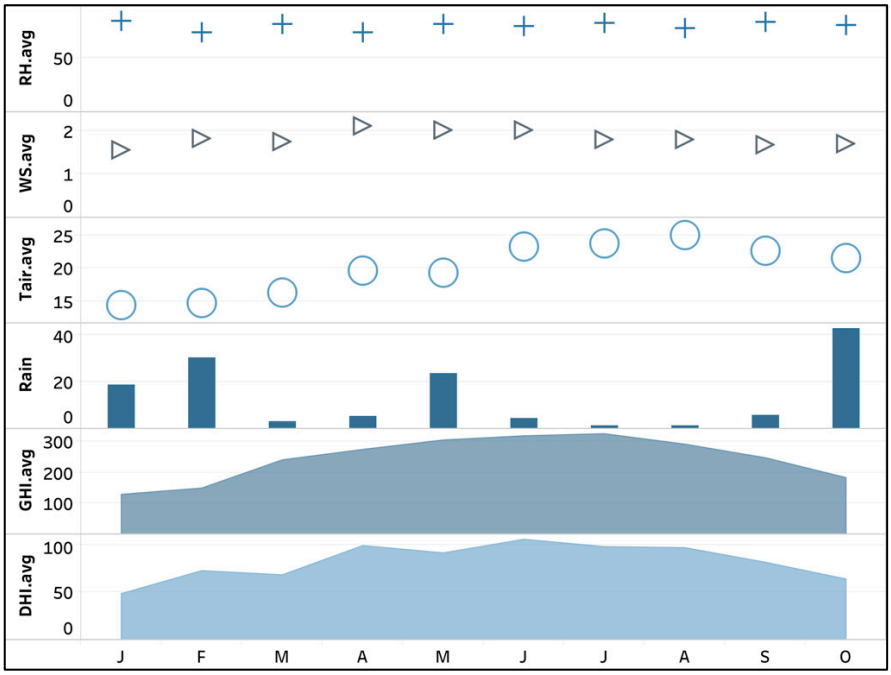

Figure 4. Average monthly distribution of variables in Rabat from January to October 2023: GHI/DHI [W/m^2], rainfall [mm/month], Tair [°C], Ws [m/s], and RH [%], (Symbols (plus, circle, triangle) are used for visual distinction between data series and do not indicate any physical meaning).

2.2. PM Monitoring and Measurements

Aerosol particle size distribution is one of the most critical physical parameters of aerosols. It defines the aerosol sedimentation velocities, lifetime in the atmosphere, and largely controls the aerosol radiative effect. Methods for measuring airborne particles can be divided into several categories. This classification actually refers to basic physical principles

or measurement approaches [25]. Figure 5 illustrates the general classification with the factor concerned for each approach. Gravimetric sampling can be based on different types of weighing. These include filter weighing—which involves weighing the sampled particles using a balance—inertial weighing using an impactor, and dynamic weighing using an oscillating microbalance [26]. Optical assessment of airborne particles is recognized as a reliable approach for characterizing airborne particles and has several important benefits. Firstly, great sensitivity to small particles, especially fine PM2.5 particles, is provided by optical detection methods such as the airborne particle analyzer. Furthermore, the optical method makes it possible to quantify particle concentrations in real time, which is crucial for ongoing air quality monitoring.

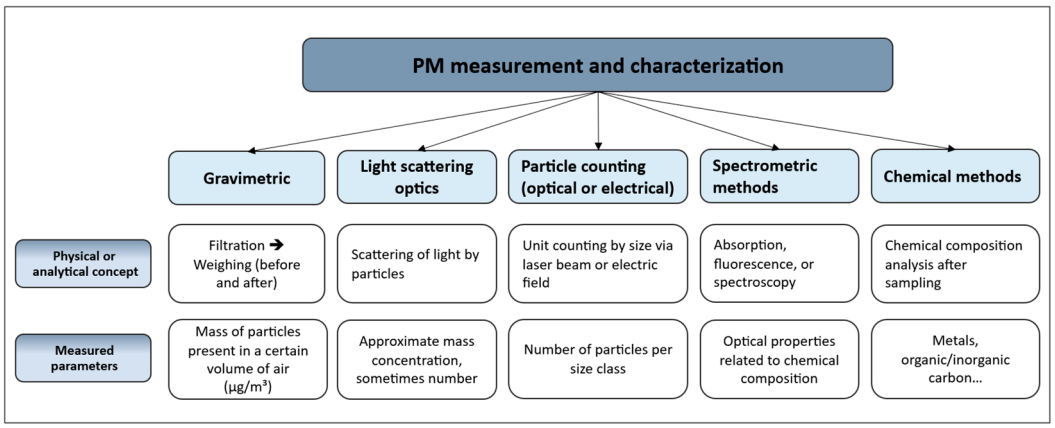

Figure 5. Classification of measurement and characterization techniques for suspended particles.

Air quality experts affirm that optical measurement tools generally cover a wide range of particle sizes, from nanometers to tens of micrometers, which is crucial for the complete characterization of aerosols. In addition, some optical instruments allow several particle characteristics to be measured simultaneously (size, concentration, and shape), providing a richer analysis [6].

2.2.1. DustTrak Functioning

The instrument used in this study was the DustTrak DRX 8533 desktop monitor. The suspended particle measurement procedure starts with the suction of aerosols through the inlet port in a continuous flow using a 3 L/min total flow pump as shown in Figure 6. First, a 1 L/min portion of the aerosol flow is divided upstream to pass through a HEPA (High-Efficiency Particulate Air) filter with a high filtration capacity for small particles, which is able to collect a significant amount of dust of about 50 mg. After this filtration, the clean air is redirected to the optical chamber as a sheath flow that effectively avoids particle recirculation to protect the optics from particle contamination. The flow of 2 L/min laden with particles leads directly into the optical chamber. At this level, the particles are illuminated by a laser beam with a wavelength of 655 nm emitted by a laser diode passing through a collimating lens and then through a cylindrical lens to generate a thin light. By measuring the amount of light re-emitted by particles, the optical sensor quantifies the concentration of airborne particles by converting the light signal into an electrical signal via the photodetector. At this level, a DC voltage offset is used internally to maintain the precision and linearity of the photometric measurements. Separately, the single-particle pulse height analyzer "SPHA" is used to analyze individual particles according to their height. At the exit of the optical chamber, there is an internal filter system where the particles can be collected for gravimetric or chemical composition analysis depending on

the type of filters inserted. Thus, a feedback loop between the pump and the flowmeter controls the entire flow rate of 3 L/min.

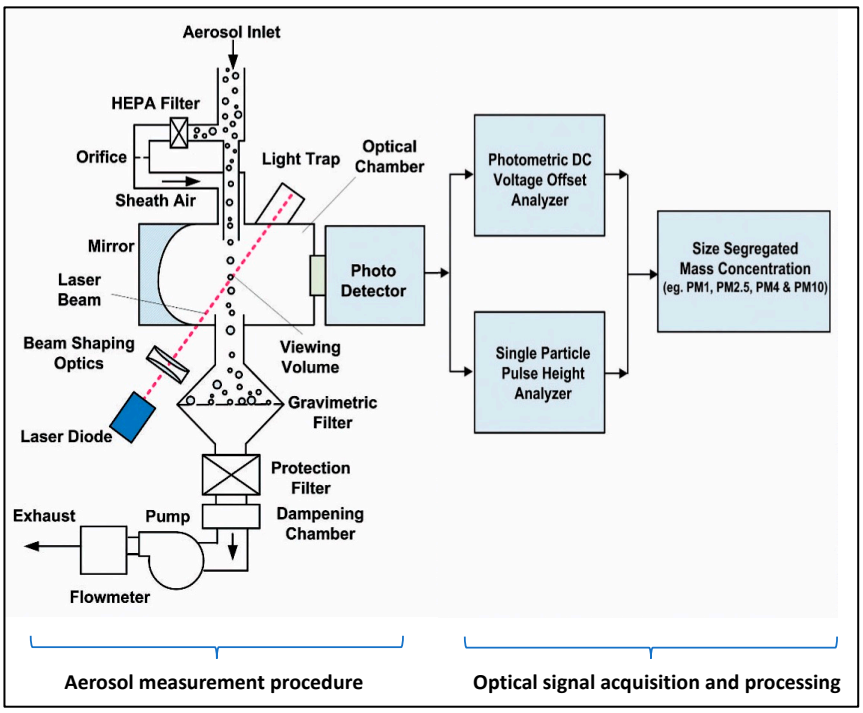

Figure 6. Schematic diagram of the aerosol measurement procedure including the acquisition and processing of the optical signal.

2.2.2. DustTrak Calibration

The DustTrak DRX monitor was calibrated by the manufacturer on November 4, 2022. Once the device was reinstalled at our location, the measured concentrations were abnormally low, not exceeding 20 $\mu m/m^3$, even on days with visible haze and apparent pollution. This observation revealed the need for in situ calibration in order to adapt the monitor and adjust it to the real environmental conditions at the site, taking into account that the type of dust at the study site differs from that used to calibrate the instrument at the original site, as represented in Table 1. Therefore, a dedicated calibration procedure was established prior to the launch of the measurement campaign. Additionally, periodic recalibrations were scheduled, according to the frequency recommended by the manufacturer, to ensure the reliability of the collected data.

Table 1. Difference between the properties of Arizona dust (24) and Rabat dust.

Reference	Origin	Shape	Density	Color	Local Representation
Arizona Dust	Synthetic/compliant with standards (ISO 12103-1) [24]	Largely angular and regular	Approximately 2.65 g/cm^3	Light brown to beige	Not related to a specific climate or pollution
Rabat Dust	Natural (urban + desert + anthropogenic)	Irregular	Depending on mineral origin	Light brown, grayish, occasionally blackish	Typical of arid/maritime climate

As previously mentioned, the monitor combines two counting techniques, namely photometry and individual size separation for mass measurement. For this purpose, the

instrument setup has two calibration factors. First, a photometer-related calibration factor, noted PCF, which considers the difference in photometric response between the measured aerosol and test dust "A1"—referring to Arizona Road Dust [24]. Secondly, a size-related calibration factor, noted SCF, which represents the differences between aerodynamic size and optical response.

Standard calibration: The standard calibration is a relatively simple protocol and does not require any external gravimetric sampling process. The procedure is carried out according to the instructions on the monitor's graphical interface and takes from 4 to 40 min. As noted previously, the size correction factor is determined to better optimize the relative accuracy of the 5 mass channels.

Advanced calibration: Advanced calibration, as the name suggests, is adopted to achieve a higher accuracy of mass concentration for all fractions. However, its application essentially requires two external gravimetric reference measurements—the first with a PM2.5 inlet impactor to establish the PCF calculated from Equation (1).

$$PCF_{new} = \frac{PM2.5_{grav}}{PM2.5_{DRX}} \text{x } PCF_{old} \quad (1)$$

where

- PCF_{new} and PC_{Fold} are the new and old SCF values, respectively;
- $PM2.5_{grav}$ and $PM2.5_{DRX}$ are the PM2.5 concentrations by gravimetric and DustTrak monitor, respectively.

The advanced calibration method was used to achieve high accuracy of size-separated mass concentration for the size fractions PM1.0, PM2.5, Respirable, and PM10. In order to carry out any gravimetric measurement, it is imperative to take into account the standard UNI EN 12,341 [12] related to gravimetric measurement. It is a European standard that combines the previous European Standards EN 12,341 (1998) and EN 14,907 (2005) [12] and describes a standardized method for determining the mass concentrations of PM10 or PM2.5 in ambient air by taking the particulate matter on the filters and weighing them with a balance. In this respect, we have taken advantage of the internal part of the monitor where it is possible to insert a filter for simultaneous internal gravimetric measurement. The measurements are performed with a PM2.5 sampling head over a nominal sampling time of 24 h. The filters used are glass microfiber filters with a diameter of 37 mm and a porosity of 1 µm, which were kept in a desiccator 24 h before each weighing. The mass weighing was ensured by a METLER precision balance. Consequently, the concentration by gravimetric method is calculated from Equation (2), detailed below:

$$PM2.5_{grav}\left(\frac{mg}{m^3}\right) = \frac{W_{post}(mg) - W_{pre}(mg)}{\frac{2}{3} * \frac{Flow_{DustTrak}\left(\frac{L}{min}\right)}{1000} * Total\ sample\ time\ (min)} \quad (2)$$

where

- W_{post} and W_{pre} are filter post-weight and pre-weight, respectively;
- The value 2/3 represents the flow used for gravimetric analysis (since 1/3 is used as sheath flow).

2.3. Particle Characterization

For the sampling of particles, glass slides of dimension 20 mm × 25 mm × 1 mm (width, length, and thickness) were exposed to the open air for two months close to the DustTrak instrument, enabling airborne particles to be captured. Scanning Electron Microscopy (SEM), Energy Dispersive X-Ray Spectroscopy (EDS), inductively coupled plasma mass spectroscopy (ICP-MS) and X-Ray diffraction analysis (XRD) are the most

common methods used in particle characterization studies [27,28]. In our case, scanning electron microscopy (SEM) was performed using a Quanta 650 model (Thermo Fisher Scientific, Waltham, MA, USA) equipped with an Apollo SDD EDS detector, to visualize the morphology and distribution of particles on the slides and also to identify the main chemical elements involved. The aim of this approach was to complete the overview of suspended particle monitoring by providing an insight into their elemental composition along with their size range, validating what was measured by the optical monitor.

2.4. Analysis of Weather Factors' Impact

The investigation into the influence of weather factors on fine particle concentrations is a highly complex issue, involving a multitude of interrelated interactions between variables. The phenomenon is multidimensional, with direct, indirect, or combined effects, making its interpretation particularly challenging. This makes it crucial to differentiate between simple statistical correlation and causal or functional dependence as weak or absent correlations can hide real influences in complex dynamics.

Initially, a preliminary assessment of linear relationships was performed to identify the limitations of classical approaches. It revealed the importance of using machine learning methods for handling non-linear relationships, such as the random forest (RF) method. This approach, broadly applied in data science, is significantly effective for processing complex systems involving numerous explanatory variables that are correlated or non-linearly related to the targeted variable. RF works by building a bunch of decision trees from random subsamples of the data, then combining their predictions to make the model more reliable and accurate. The importance evaluation in our study relies on a permutation approach: the model performance is measured after randomly disturbing the values of a selected variable. A substantial drop in performance reveals a significant role of this variable in the estimation. This permits estimating the relative contribution of each meteorological factor to the observed variability, addressing interdependencies and multiple interactions. The modeling was implemented in Python (version 3.10), within a Jupyter Notebook environment, including data preprocessing such as cleaning, normalization, and feature selection. The analysis was conducted separately for each city in order to account for local specificities.

3. Results and Discussion

3.1. Dust Trak Calibration

A mixed calibration approach has been chosen to ensure that both factors are calibrated. In the first step, the calibration of the first SCF factor is carried out using the standard calibration performed at the instrument settings level using Equation (1), which is illustrated in Figure 7a. In a second step, with the availability of the 2.5 input impactor, the gravimetric protocol was carried out with the calculation of several PM2.5 concentrations based on Equation (3) to derive an average to be used in Equation (2). The new calibrated factors are shown in the table in Figure 7b.

(**a**)

(**b**)

	Default value	Adjusted value
SCF	1.00	1.30
PCF	1.00	1.02

Figure 7. (**a**) Graphical interface of the monitor showing the new SCF established after the standard calibration; (**b**) table of adjusted calibration values.

3.2. PM Exploratory Data Analysis (EDA)

Continuous data collection is essential for an accurate representation of air pollution as it can identify not only general trends but also short-term fluctuations. Relevant factors are grouped in Table 2 for the assessment of measurements of variability and homogeneity of all variables in the two regions. PM2.5 particles are a subset of PM10 particles, and both generally follow similar trends. The considerable degree of correlation between mean and median values indicates that the data are not significantly affected by outliers, thereby reinforcing the reliability of the mean as an indicator of central tendency.

Table 2. Descriptive statistics of daily mean values of environmental variables [$\mu m/m^3$] and meteorological variables for Rabat and Marrakech regions.

	Variable	Mean	Min	Max	Median	SD	Asymmetry
RABAT	**PM2.5 [$\mu m/m^3$]**	42.24	16.3	125.9	42.00	14.68×10^{-4}	0.46
	PM10 [$\mu m/m^3$]	43.27	16.3	127.6	42.86	16.01×10^{-4}	0.42
	Tair [°C]	19.97	17.22	22.45	19.89	1.90	−0.02
	RH [%]	79.14	68.53	89.03	8061	7.55	−0.14
	WS [m/s]	1.83	0.11	11.19	1.66	1.05	1.11
MARRAKECH	**Variable**	**Mean**	**Min**	**Max**	**Median**	**SD**	**Asymmetry**
	PM2.5 [$\mu m/m^3$]	6.18	1.50	25.58	5.43	3.37	1.62
	PM10 [$\mu m/m^3$]	17.74	4.72	42.94	16.89	7.64	0.75
	Tair [°C]	21.13	9.25	36.38	21.71	5.53	0.01
	RH [%]	54.95	20.94	84.02	56.12	1309	−0.18
	WS [m/s]	1.96	0.85	4.96	1.91	0.53	1.29

For the Rabat region, continuous real-time data collected from 3 January to 3 November 2023 were used. Measurements were taken at regular 15 min intervals, providing a precise and detailed record of variations in PM concentrations over this period. The low values of the standard deviation of PM10 and PM2.5 concentrations—which quantifies the dispersion

of measured values around the mean—imply relatively constant particle levels over time. Furthermore, asymmetry or skewness indicates the degree to which a distribution deviates from symmetry. It can be stated that a distribution is asymmetric if it is not symmetrical around its mean. For the positive values shown, we can say that the tail of the distribution extends to the right, meaning that the majority of values are concentrated on the left of the mean. An extreme value was determined by comparing the aggregated benchmark with and without the extreme value. In particular, the month of February includes two extreme values recorded on February 18, possibly linked to the gardening activity at the institution. It is true that eliminating these two values will significantly lower the average monthly trend; however, we did not proceed that way in order to highlight the link between any such activity and the high concentration levels. During the month of February, the monthly average concentration of PM2.5 and PM10 reached a worrying level of 75 µm/m^3, which is the highest value for the study period (Figure 8).

Figure 8. Concentrations of PM2.5 and PM10 [mg/m^3] (**a**) over Rabat region, (**b**) over Marrakech region.

In the city of Marrakech, seasonal variations were observed, with higher levels and greater variability in the middle of the year (May–September) and a slight decrease at the end of 2024 (November–December). Values of PM2.5 are generally lower than PM10 values, remaining mostly below 0.015 mg/m^3, while the PM10 peaks and intensity suggest that coarse particles are likely to be dominant.

In fact, seasonality represents a crucial factor in the dynamics of suspended particulate concentrations. Although particle size does not change proportionally with the seasons, seasonal variations in emission sources, meteorological conditions, and transport mechanisms influence the concentration and distribution of airborne particles. The impact of seasonal variations affects fine and coarse particles differently [27]. For example, fine particles, having a lighter weight, can remain suspended in the air for longer and are more susceptible to atmospheric stagnation conditions, such as those observed in winter. Moreover, seasonal variations can be further affected by human activities, which vary from season to season. The increased use of heaters in winter can increase particulate emissions, while agricultural activities in spring can similarly contribute to pollution peaks.

3.3. Particle Characterization

Knowledge of the constituents of suspended particles provides valuable information on the types of contaminants present. SEM images allow us to characterize particle morphology in terms of size, shape, and surface. The images (see Figure 9) reveal a variety of morphologies, with diameters ranging from 1 to 15 µm, along with aggregates reaching over 20 µm. Shapes tend to be geometrically spherical or elliptical, noting that the morphology of each particle is strongly linked to its deposition on the glass surface. Aggregates of this kind could indicate cross-particle interactions or the effect of humidity and other atmospheric conditions on particle coagulation. These observations suggest heterogeneity in particle size and shape, reflecting their multifactorial origin. A previous study performed by our research team revealed that particle size distribution was broadest in the range of 3 to 14 µm with significant concentration in the 3–7 µm range [29]. This result is consistent with current SEM images, which show a preponderance of fine particles, often involved in atmospheric deposition and soiling processes. Furthermore, the rounding shapes may be characteristic of particles from industrial or combustion processes, while oval and more irregular particles may come from mineral dust or marine aerosols [30].

Semi-quantitative elemental analysis carried out on several slides taken from the same area (Figure 10) shows a chemical composition based on mineral and metallic elements. The high oxygen (O) content associated with silicon (Si), aluminum (Al), iron (Fe), and calcium (Ca) could suggest the presence of mineral dust or building materials. As a matter of fact, iron is often present in mineral dusts and vehicle abrasion particles. In addition, a peak of Si frequently indicates the presence of terrestrial dust and sand as the latter is one of the main components of silicates, the building blocks of rocks and soils. Titanium can indicate the existence of specific materials, such as pigments or particles derived from the degradation of titanium-containing materials. Furthermore, it can even influence particle properties, particularly in terms of chemical reactivity and environmental behavior. For example, Ti can interact with other contaminants and influence their transport [31]. On the other hand, Mg and Na are generally attributed to marine salts [32]. Their presence in atmospheric particles may indicate a marine influence, especially if the sample is taken in a coastal area such as Rabat. In addition to their marine origin, they may also be present in certain mineral particles.

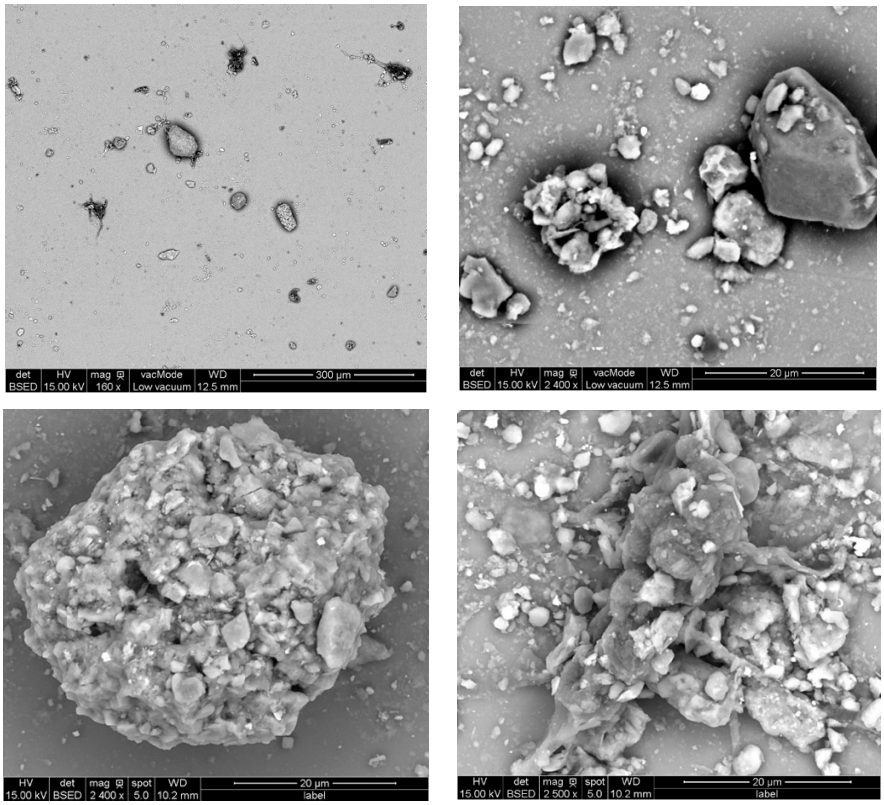

Figure 9. Various SEM images of particles at 160× and 2400× magnification.

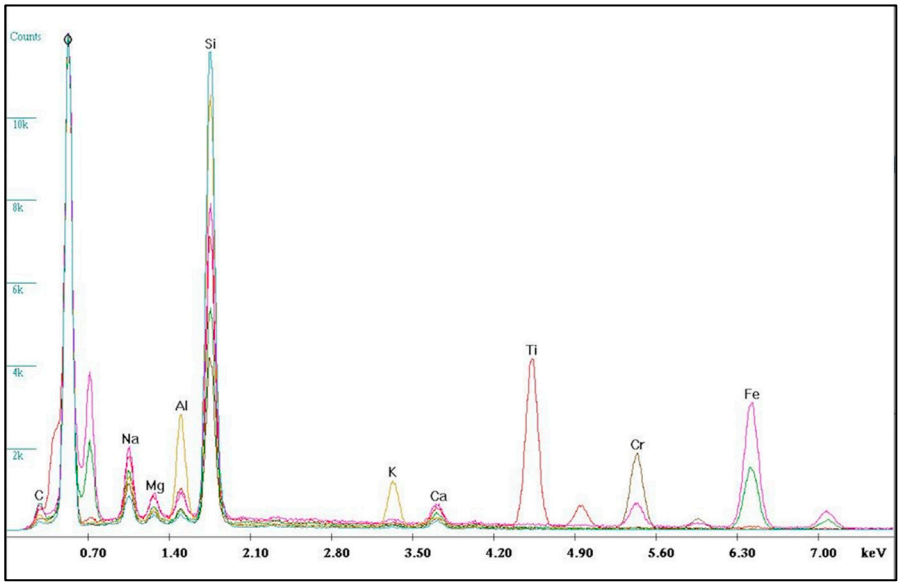

Figure 10. Superposition of EDS spectra on several slides for Rabat region.

3.4. Analysis of Weather Factors' Impact

3.4.1. Heat Map and Hourly Profile

Atmospheric particle concentrations largely depend on the quantity of particles emitted by various sources, along with local and regional meteorological conditions that influence pollutant dispersion and deposition on the ground [33]. The heat map presented in Figure 11 illustrates the correlation level between PM concentrations and various meteorological variables. It seems that the relationship between these variables is not necessarily

linear, as evidenced by a low Pearson's correlation coefficient. The strong correlation between PM2.5 and PM10 can be seen first, prompting us to retain the PM10 concentration for further interpretation. A negative correlation is found between air temperature and time.

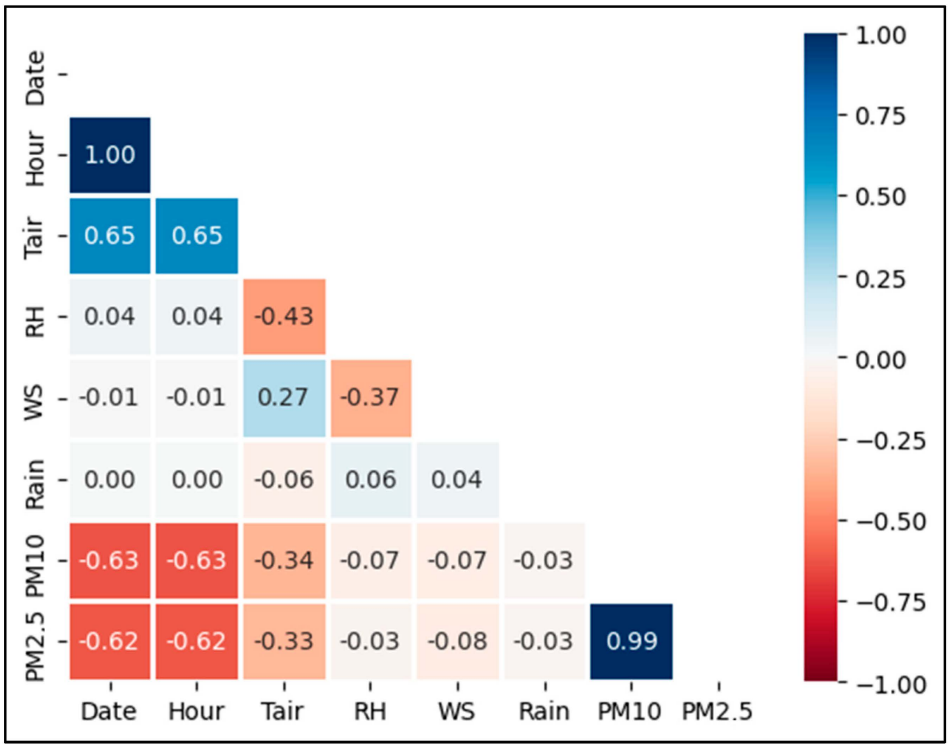

Figure 11. Heat map charting the level of correlation between PM concentrations and various meteorological variables.

The concentration and behavior of particles differ during the day and at night. In order to improve our understanding of variations in PM concentrations over the course of the day, hourly time-series monitoring was adopted. The diagram (Figure 12) plots the hourly average of PM10 concentrations. The exceedance occurs at two key times of the day: between 8 and 11 a.m. and from 7 to 10 p.m. These periods correspond to peaks in human activity; in particular, rush hours associated with traffic and increased vehicle use, thus contributing to an increase in airborne particles. Additionally, wind has a considerable impact on particle dispersion. In the case of strong winds, PM can be dispersed and their concentration reduced, while weak winds or changes in direction can lead to local particle accumulation [34].

The highest PM concentration, occurring around 8 p.m., coincided with a significant drop in temperature. In some cases, this may be related to a temperature inversion phenomenon, which prevents the vertical dispersion of pollutants by trapping cold air under a layer of warmer air. This inversion leads to an accumulation of particles close to the ground [35]. Simultaneously, an increase in humidity levels is observed due to the inverse relationship between temperature and humidity. This increase can not only reinforce the effect of the inversion but also encourage the condensation of fine particles, making them larger and more concentrated in the air [35,36]. The above phenomenon contributes significantly to the elevation of PM levels during this period.

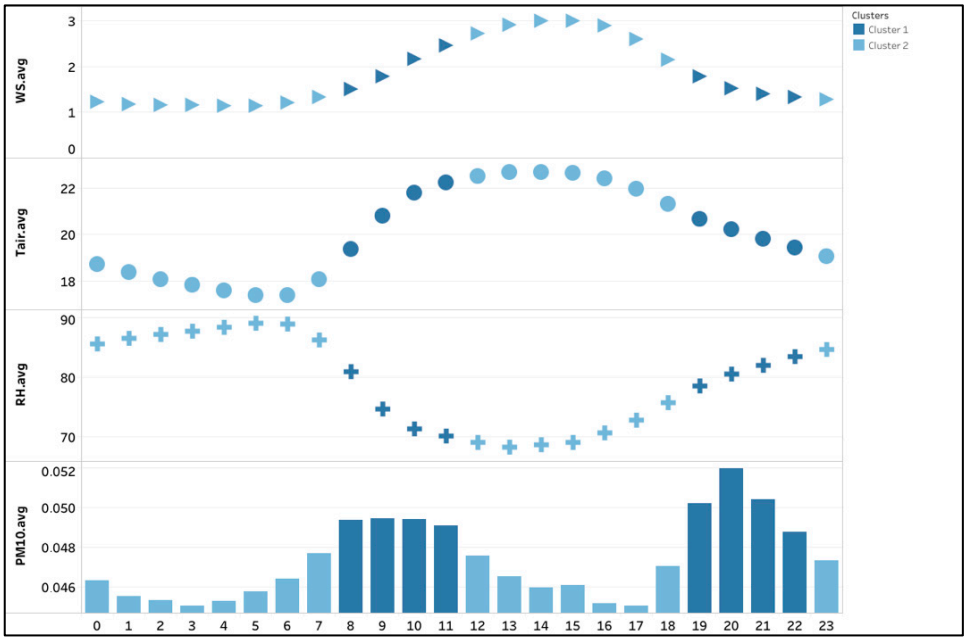

Figure 12. Hourly profile of PM10 concentrations [mg/m^3], wind speed [m/s], temperature [°C], and relative humidity [%].

3.4.2. Analysis by Random Forest Method

According to the findings presented in the analysis, the meteorological variables influencing PM10 concentrations vary depending on the climatic characteristics of the two cities. As represented in Figure 13, the ambient temperature (Tair) is by far the most influential variable in Rabat (>35%), while in Marrakech, it is still significant but slightly less dominant. Potentially, PM concentrations can be influenced by the phenomenon of temperature inversion, as mentioned in the previous section, as well as the influence of temperature levels on the physico-chemical reactions involved in the formation of PM10. Wind speed and direction are of moderate importance in both environments, showing their role in particle dispersion and long-distance transportation. Similarly, relative humidity plays an intermediate role in both situations. It influences the condensation and aggregation of particles, thereby affecting the dynamics of PM10 in the atmosphere. With its semi-arid climate and high levels of sunshine, the strongest influence for the city of Marrakech is from solar irradiance (DHI and GHI), which suggests a role for photo-chemical processes in the generation and transformation of PM10.

A noteworthy discrepancy is the low influence of rainfall in the city of Rabat, which is rather surprising given the general expectation of a contribution from rainfall to the leaching of PM. In Marrakech, however, rain makes a greater impact, which may be attributed to the larger effect of atmospheric cleaning in a semi-arid environment where rain is less frequent but more effective when it does occur.

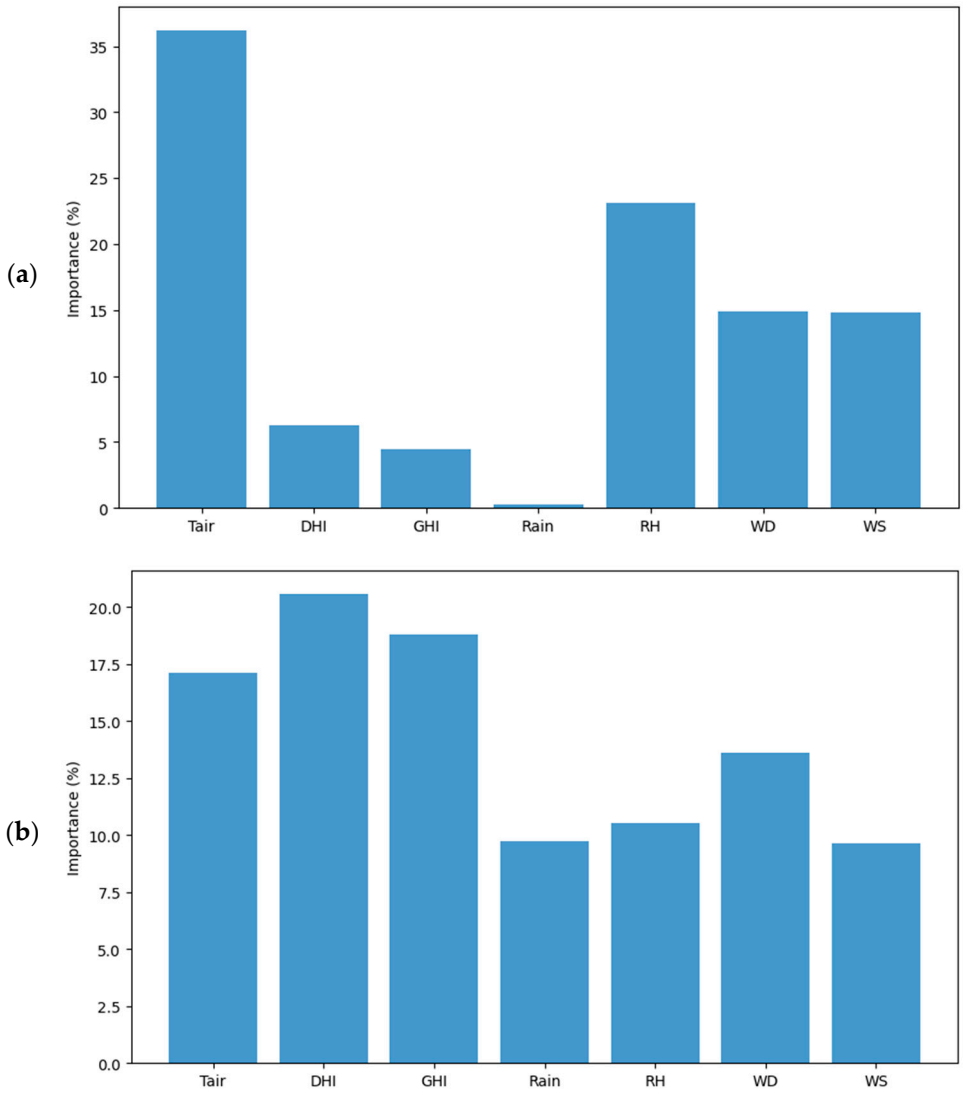

Figure 13. Importance of weather's vectors relating to PM10 concentration (**a**) for Rabat's site; (**b**) for Marrakech's site.

4. Conclusions

The ultimate aim of this research was the continuous, real-time monitoring of PM concentrations using an optical monitor providing a distribution by aerodynamic diameter size. Before launching this tracking, it was essential to calibrate the instrument in question to ensure the reliability and accuracy of the measurements. The internal functioning as well as the on site calibration protocol adopted are presented in detail.

Over the study period in Rabat City, from January to October 2023, PM2.5 and PM10 concentrations demonstrated significant variations. According to the results obtained, the highest PM concentrations generally occur around 8 p.m., a period that corresponds to a high level of relative humidity and low wind speed. These conditions tend to favor the accumulation of PM in the air, and the PM dispersion also depends on the stability of the atmosphere. Additionally, physico-chemical analysis of particles deposited on glass slides provided an insight into their morphology and composition. The dominating elements, such as O, Si, and Fe, suggest terrestrial or industrial sources, while the presence of sodium and magnesium indicates a marine influence.

Concerning the evaluation of the importance of weather variables in relation to PM concentrations, the use of the random forest method for data from two distinct envi-

ronments allowed for the identification of similarities and differences in the influential variables. In Rabat, temperature and humidity are the prevailing factors, in line with the moderating effect of the Atlantic Ocean. In Marrakech, solar irradiance and rain play a more important role, highlighting the effect of the arid climate and intense sunshine on the dynamics of PM10. In terms of physical and atmospheric trends, the city of Rabat, given its proximity to the ocean, is clearly influenced by temperature and relative humidity, which affect the dynamics of PM10 through the absorption of water and variations in atmospheric chemical reactions.

The findings reveal PM fluctuations and trends for the city of Rabat, especially given the remarkable lack of similar data at the national level. At the same time, it sheds light on the relationship between PM concentration and meteorological variables, which collectively govern the energy production of solar installations. Overall, data and conclusions from this study are of crucial importance for the modeling of soiling.

Author Contributions: S.Z.: Conceptualization, Methodology, Formal Analysis, Data Curation, Writing—Original Draft, Investigation. B.L.: Conceptualization, Methodology, Investigation, Review and Editing. H.C.: Conceptualization, Investigation. A.D.: Methodology, Resources, Validation, Data Curation, Supervision, Review and Editing. A.A.: Conceptualization, Validation, Supervision. K.R.: Validation. A.B.: Methodology, Validation, Review and Editing, Funding Acquisition, Project Administration, Supervision, M.T.: Validation, Supervision, Funding Acquisition, Review and Editing. All authors have read and agreed to the published version of the manuscript.

Funding: The work is funded by national funds through FCT—Fundação para a Ciência e Tecnologia, I.P., in the framework of the CREATE project and through GRASP-SYNERGY (Grant Agreement Project 101131631), UniversaPulsar, GRASP-Synergy and The Moroccan Ministry for Higher Education, Scientific Research, and Innovation in the framework of Priority Research Project PPR1 Nr. 14/2016.

Data Availability Statement: Data set available upon request from the authors. Other data are exported from the Worldwide Air Quality platform, AirNet Sensor Network.

Acknowledgments: The authors would like to thank M.M. Rhafiri and M.G. El Moutawakil for their invaluable help and pertinent remarks.

Conflicts of Interest: The authors declare no conflicts of interest.

References

1. Guan, J.; Dai, Z.; Wang, R.; Zhang, C.; Chen, S.; Guo, Y.; Zhang, X.; Wu, Y. Pollution characteristics and control strategies of typical waste plastic recycling plants. *J. Environ. Chem. Eng.* **2025**, *13*, 1169398. [CrossRef]
2. Niu, X.; Yu, J.; Sun, J.; Zhang, X.; Zhou, L.; Liu, X.; He, K.; Peng, Z.; Niu, X.; Xu, H.; et al. New mechanisms of $PM_{2.5}$ induced atherosclerosis: Source dependent toxicity and pathogenesis. *Environ. Res.* **2024**, *266*, 120535. [CrossRef]
3. Inomata, Y.; Matsuki, A.; Kajino, M.; Kaneyasu, N.; Seto, T. Decreasing trends in $PM_{2.5}$ and BC concentrations observed on central and southwestern Japanese Islands. *Atmos. Pollut. Res.* **2024**, *15*, 102258. [CrossRef]
4. Yeo, Y.H.; Gawk, M.A.; Lee, S.Y.; Nam, Y.S.; Park, W.H. Air purifier using super-absorbent polymer for removing air contaminants. *J. Environ. Chem. Eng.* **2022**, *10*, 107832. [CrossRef]
5. Nazneen; Patra, A.K.; Kolluru, S.S.R.; Penchala, A.; Kumar, S.; Mishra, N.; Sree, N.B.; Santra, S.; Dubey, R. Assessment of seasonal variability of PM, BC and UFP levels at a highway toll stations and their associated health risks. *Environ. Res.* **2023**, *245*, 118028. [CrossRef] [PubMed]
6. Dewage, P.M.H.; Wijeratne, L.O.H.; Yu, X.; Iqbal, M.; Balagopal, G.; Waczak, J.; Fernando, A.; Lary, M.D.; Ruwali, S.; Lary, D.J. Providing Fine Temporal and Spatial Resolution Analyses of Airborne Particulate Matter Utilizing Complimentary In Situ IoT Sensor Network and Remote Sensing Approaches. *Remote Sens.* **2024**, *16*, 2454. [CrossRef]
7. Cao, J.; Chow, J.C.; Lee, F.S.C.; Watson, J.G. Evolution of $PM_{2.5}$ measurements and standards in the U.S. and future perspectives for China. *Aerosol Air Qual. Res.* **2013**, *13*, 1197–1211. [CrossRef]
8. Directive, C. Relating to limit values for sulphur dioxide, nitrogen dioxide and oxides of nitrogen, particulate matter and lead in ambient air. *Off. J. Eur. Communities* **1999**, *163*, 41–60.

9. Word Health Organization. *World Health Statistics 2024: Monitoring Health for the SDGs, Sustainable Development Goals*; Word Health Organization: Geneve, Switzerlan, 2024.
10. Kung, H.-C.; Uyen, T.P.; Huang, B.-W.; Mutuku, J.K.; Chang-Chien, G.-P. Evaluation of tire wear particle concentrations in TSP and PM_{10} using polymeric and molecular markers. *Process. Saf. Environ. Prot.* **2024**, *184*, 342–354. [CrossRef]
11. Wang, F.; Cen, K.; Li, N.; Huang, Q.; Chao, X.; Yan, J.; Chi, Y. Simultaneous measurement on gas concentration and particle mass concentration by tunable diode laser. *Flow. Meas. Instrum.* **2010**, *21*, 382–387. [CrossRef]
12. Wang, Z.; Calderón, L.; Patton, A.P.; Allacci, M.S.; Senick, J.; Wener, R.; Andrews, C.J.; Mainelis, G. Comparison of real-time instruments and gravimetric method when measuring particulate matter in a residential building. *J. Air Waste Manag. Assoc.* **2016**, *66*, 1109–1120. [CrossRef] [PubMed]
13. Valerino, M.; Ratnaparkhi, A.; Ghoroi, C.; Bergin, M. Seasonal photovoltaic soiling: Analysis of size and composition of deposited particulate matter. *Sol. Energy* **2021**, *227*, 44–55. [CrossRef]
14. Penchala, A.; Patra, A.K.; Mishra, N.; Santra, S. Field calibration and performance evaluation of low-cost sensors for monitoring airborne PM in the occupational mining environment. *J. Aerosol Sci.* **2025**, *184*, 106519. [CrossRef]
15. Scherließ, R. Chapter 22: Particle Size Measurements in Aerosols. In *Analytical Techniques in the Pharmaceutical Sciences*; Springer: Berlin/Heidelberg, Germany, 2016; pp. 701–715.
16. Carter, R.M.; Yan, Y.; Cameron, S.D. On-line measurement of particle size distribution and mass flow rate of particles in a pneumatic suspension using combined imaging and electrostatic sensors. *Flow Meas. Instrum.* **2005**, *16*, 309–314. [CrossRef]
17. Obregón, M.; Costa, M.; Silva, A.; Serrano, A. Impact of aerosol and water vapour on SW radiation at the surface: Sensitivity study and applications. *Atmospheric Res.* **2018**, *213*, 252–263. [CrossRef]
18. Hosseini Dehshiri, S.S.; Firoozabadi, B. Dust cycle, soiling effect and optimum cleaning schedule for PV modules in Iran: A long-term multi-criteria analysis. *Energy Convers. Manag.* **2023**, *286*, 117084. [CrossRef]
19. Chamali, H.; Dahrouch, A.; Laarabi, B.; Fathi, E.H.; Barhdadi, A. Evaluating the distribution of soil particle size on glass samples by a new generation of optical microscopy for solar PV applications. *Environ. Sci. Pollut. Res.* **2022**, *30*, 81686–81696. [CrossRef]
20. Millet, T.; Bencherif, H.; Bounhir, A.; Bègue, N.; Lamy, K.; Ranaivombola, M.; Benkhaldoun, Z.; Portafaix, T.; Duflot, V. Aerosol Distributions and Transport over Southern Morocco from Ground-Based and Satellite Observations (2004–2020). *Atmosphere* **2022**, *13*, 923. [CrossRef]
21. Micheli, L.; Muller, M. An investigation of the key parameters for predicting PV soiling losses. *Prog. Photovolt. Res. Appl.* **2017**, *25*, 291–307. [CrossRef]
22. Son, J.; Jeong, S.; Park, H.; Park, C.-E. The effect of particulate matter on solar photovoltaic power generation over the Republic of Korea. *Environ. Res. Lett.* **2020**, *15*, 084004. [CrossRef]
23. Tamoor, M.; Hussain, M.I.; Bhatti, A.R.; Miran, S.; Arif, W.; Kiren, T.; Lee, G.H. Investigation of dust pollutants and the impact of suspended particulate matter on the performance of photovoltaic systems. *Front. Energy Res.* **2022**, *10*, 1017293. [CrossRef]
24. Javed, W.; Guo, B. Performance Evaluation of Real-time Dust Trak Monitors for Outdoor Particulate Mass Measurements in a Desert Environment. *Aerosol Air Qual. Res.* **2021**, *21*, 1. [CrossRef]
25. Kumar, A.; Dhawan, S.; Kumar, M.V.; Khare, M.; Nagendra, S.S.; Dubey, S.K.; Mehta, D.S. Detection and identification of shape, size, and concentration of particulate matter in ambient air using bright field microscopy-based system. *Atmos. Pollut. Res.* **2023**, *14*, 101913. [CrossRef]
26. Vasilatou, K.; Iida, K.; Kazemimanesh, M.; Olfert, J.; Sakurai, H.; Sipkens, T.A.; Smallwood, G.J. Aerosol physical characterization: A review on the current state of aerosol documentary standards and calibration strategies. *J. Aerosol Sci.* **2024**, *183*, 106483. [CrossRef]
27. Pipal, A.S.; Jan, R.; Satsangi, P.G.; Tiwari, S.; Taneja, A. Study of surface morphology, elemental composition and origin of atmospheric aerosols ($PM_{2.5}$ and PM_{10}) over Agra, India. *Aerosol Air Qual. Res.* **2014**, *14*, 1685–1700. [CrossRef]
28. Longoria-Rodríguez, F.E.; González, L.T.; Mancilla, Y.; Acuña-Askar, K.; Arizpe-Zapata, J.A.; González, J.; Kharissova, O.V.; Mendoza, A. Sequential SEM-EDS, PLM, and MRS Microanalysis of Individual Atmospheric Particles: A Useful Tool for Assigning Emission Sources. *Toxics* **2021**, *9*, 37. [CrossRef] [PubMed]
29. Laarabi, B.; El Baqqal, Y.; Dahrouch, A.; Barhdadi, A. Deep analysis of soiling effect on glass transmittance of PV modules in seven sites in Morocco. *Energy* **2020**, *213*, 118811. [CrossRef]
30. Sielicki, P.; Janik, H.; Guzman, A.; Namieśnik, J. The Progress in Electron Microscopy Studies of Particulate Matters to Be Used as a Standard Monitoring Method for Air Dust Pollution. *Crit. Rev. Anal. Chem.* **2011**, *41*, 314–334. [CrossRef]
31. Dylla, H.; Hassan, M.M.; Mohammad, L.N.; Rupnow, T.; Wright, E. Evaluation of Environmental Effectiveness of Titanium Dioxide Photocatalyst Coating for Concrete Pavement. *Transp. Res. Rec.* **2010**, *2164*, 46–51. [CrossRef]
32. Javed, W.; Guo, B. Chemical characterization and source apportionment of fine and coarse atmospheric particulate matter in Doha, Qatar. *Atmos. Pollut. Res.* **2021**, *12*, 122–136. [CrossRef]
33. Javed, W.; Guo, B.; Figgis, B. Modeling of photovoltaic soiling loss as a function of environmental variables. *Sol. Energy* **2017**, *157*, 397–407. [CrossRef]

34. Yang, Z.; Yang, X.; Xu, C.; Wang, Q. The Effect of Meteorological Features on Pollution Characteristics of $PM_{2.5}$ in the South Area of Beijing, China. *Atmosphere* **2023**, *14*, 1753. [CrossRef]
35. Lagmiri, S.; Dahech, S. Temperature Inversion and Particulate Matter Concentration in the Low Troposphere of Cergy-Pontoise (Parisian Region). *Atmosphere* **2024**, *15*, 349. [CrossRef]
36. Glojek, K.; Močnik, G.; Alas, H.D.C.; Cuesta-Mosquera, A.; Drinovec, L.; Gregorič, A.; Ogrin, M.; Weinhold, K.; Ježek, I.; Müller, T.; et al. The impact of temperature inversions on black carbon and particle mass concentrations in a mountainous area. *Atmos. Chem. Phys.* **2022**, *22*, 5577–5601. [CrossRef]